

Spectral Similarity and Difference of Naphthalenetetracarboxylic Dianhydride, Perylenetetracarboxylic Dianhydride, and Their Derivatives

Masafumi Adachi,* Yukichi Murata, and Shinichiro Nakamura

Mitsubishi Chemical Corporation, Yokohama Research Center, 1000 Kamoshida-cho, Aoba-ku, Yokohama 227, Japan

Received: November 10, 1994[⊗]

Although the sizes of their π -conjugation systems are different, the absorption spectra of 1,4,5,8-naphthalenetetracarboxylic dianhydride, its diimide (NTCAI), 3,4,9,10-perylenetetracarboxylic dianhydride, and its diimide (PTCAI) show similar experimental features consisting of the main band with some subordinational bands. However, the origins of the transitions in the observed bands are reported to be quite different. In order to understand the relationship between the conjugation size and the details of the transition properties, we studied the absorption spectra of naphthalene, 1,8-naphthalenedicarboxylic anhydride imide (NDCAI), NTCAI, and PTCAI by the semiempirical MO INDO/S method. Comparison of the observed and calculated spectra showed that NDCAI and NTCAI have two π - π^* transitions that are perpendicular and close in energy. Thus the observed bands can be described by the mixing of two electronic transitions with vibronic progressions. For PTCAI the observed bands consist of one electronic transition and its vibronic progressions. The mechanism of the absorption wavelength shift from naphthalene, NDCAI, and NTCAI to PTCAI was analyzed. The π - π^* transitions with high intensity in the direction of the long axis show a remarkable bathochromic shift, due to the high content of HOMO \rightarrow LUMO excitation. The bathochromic shift is explained by the decrease of the orbital energy gap. The π - π^* transitions with low intensity in the direction of the short axis show only a small bathochromic shift, and this shift can be explained by the small change of the orbital energy gaps. The n - π^* transitions in NDCAI, NTCAI, and PTCAI were also analyzed; the absorption wavelengths of the n - π^* transitions are kept at almost the same levels for NDCAI, NTCAI, and PTCAI.

1. Introduction

Electronic transitions, which primarily determine the color of materials, are mainly controlled by the π -conjugation size. Reviews of the experimental data, the theoretical calculations, and the relationship between the size of the π -conjugation and the absorption spectra have been published.^{1–3} However, a complete understanding of the shift in the absorption spectra is still lacking. Systematic studies of the shift as a function of the π -conjugation size are quite limited. As an exception, Nishimoto has recently developed a theoretical method, which is based on the RPA (random phase approximation), that shows excellent agreement between the π -conjugation size dependences of observed and calculated absorption spectra.⁴ The basic understanding of the spectrum will provide insight into the design of organic functional materials. The current investigation was performed in order to understand how the π -conjugation size affects the electronic and spectral properties of a dye material.

Investigators have suggested methods of calculating absorption spectra of dyes and pigments from a quantum chemical point of view. One approach is to use the Pariser–Parr–Pople (PPP) method in which a π -electron approximation is adopted.^{2,3} The PPP method, however, was originally constructed for planar π -conjugated systems, and therefore it cannot be applied to nonplanar molecules, n - π^* transitions, or intermolecular interactions, such as hydrogen bonds. Another approach is to use the semiempirical MO INDO/S method,⁵ which uses all the valence electrons to predict the spectral properties of a compound. The validity of the INDO/S method has been demonstrated,⁶ and it has been used to study the mixing of π - π^*

and n - π^* excitations in nonplanar azomethine dyes,⁷ the intermolecular interaction of porphyrin,^{8a} organic dyes containing transition metals,^{8b} and the solid state absorption spectrum of 1,4-dioxo-3,6-diphenylpyrrolo[3,4-*c*]pyrrole⁹ systems. In the current study, we chose the INDO/S method for absorption spectrum calculations.

1,4,5,8-Naphthalenetetracarboxylic dianhydride (NTCA) and its diimide derivatives (NTCAI) are almost colorless and were recently applied as UV-absorbing agents in polymers because of their UV and visible absorption properties.¹⁰ On the other hand, 3,4,9,10-perylenetetracarboxylic dianhydride (PTCA) and its diimide derivatives (PTCAI) are colored and are used as high performance pigments¹¹ because of their variation of colors and fatigue resistance; moreover, they were applied recently as charge generation molecules in electrophotography.¹² These molecules are important dyes.

The absorption spectra of NTCA and NTCAI show an absorption band (300–400 nm) consisting of a few peaks and shoulders (Figure 1).¹³ The absorption spectra of PTCA and PTCAI show an absorption band (400–550 nm) also consisting of three or four peaks (Figure 2).¹⁴ From a structural point of view, the difference in NTCA and PTCA exists only in the number of naphthalene rings; consequently, differences between these two spectra would reflect the π -conjugation size effect, as a drastic change of the transition properties is not expected. However, experimental spectroscopic studies have shown completely different transition properties. Magnetic circular dichroism (MCD) measurements showed that the NTCA and NTCAI absorption band consists of two electronic transitions together with their vibronic progressions.^{13a} On the other hand, linear dichroism (LD) and circular dichroism (CD) measurements showed that the PTCA and PTCAI absorption band consists of only one electronic transition with vibronic

[⊗] Abstract published in *Advance ACS Abstracts*, September 1, 1995.

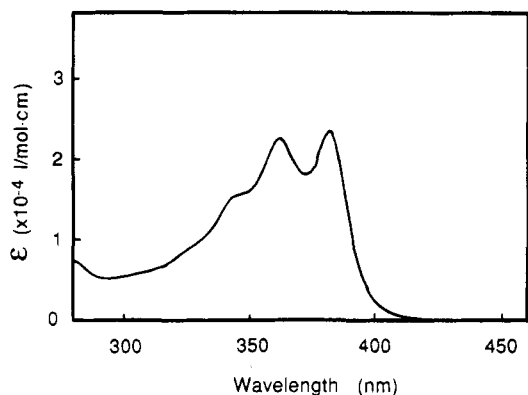


Figure 1. Absorption spectrum of *p*-COOC₂H₅-C₆H₄-NTCAI (**6**). (λ_{\max} (ϵ): 382 nm (23 600), 361 nm (22 900), 344 nm (shoulder); in DMSO solution, 5.69×10^{-5} M).

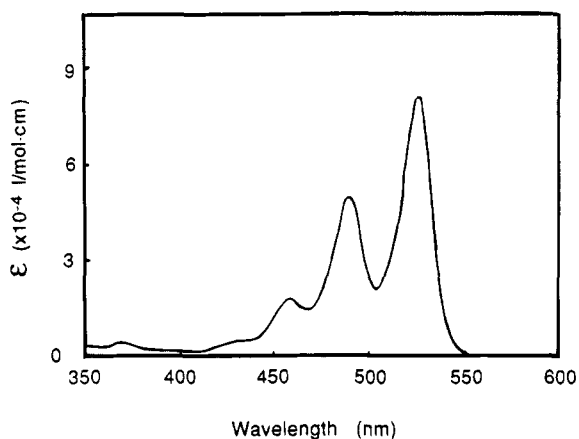


Figure 2. Absorption spectrum of *n*-C₄H₉(C₂H₅)-CHCH₂-PTCAI. (λ_{\max} (ϵ): 526 nm (81 500), 489 nm (49 400), 458 nm (18 000), 431 nm (shoulder), 370 nm (4000); in CHCl₃ solution, 1.10×10^{-5} M).

progressions.^{14c} These experimental observations provide an unique opportunity to study the origin of the interesting difference from a theoretical point of view.

Investigations on NTCA and NTCAI are limited: Yamaguchi *et al.* reported the absorption and MCD spectra and the CNDO/S-calculated transition property of NTCA and 1,8-naphthalenedicarboxylic anhydride (NDCA).^{13a} The donor-acceptor complex including NTCAI is reported by some researchers,¹⁵ especially Zsom *et al.*, who analyzed the charge-transfer absorption band by the PPP method.^{15e} Recently, Zhong *et al.* reported the imide substituent effect for the aggregation behavior.¹⁶ For NDCA and its imide derivatives (NDCAI), the absorption and the fluorescence spectra were analyzed by spectroscopy and theoretical calculations.¹⁷ Bigotto *et al.* assigned the transition bands including that for the $n-\pi^*$ transition on the basis of INDO/S calculations.^{17a} Celnik *et al.* discussed the observed substituent effect with respect to the results of PPP calculations.^{17b} Pardo *et al.* also discussed it using the CNDO/S method.^{17c} For PTCA and PTCAI, Langhals *et al.* reported the absorption, fluorescence spectra, and other properties for many kinds of imide (N-) substituents.^{14a,14c,18} PTCAI imide substituent effects for the solid state absorption spectrum and the crystal structure were summarized by Klebe *et al.*¹¹ The relationship between the xerographic sensitivity and the absorption spectrum in the solid state structure of various kinds of N-substituted PTCAI was reported by Duff *et al.*^{12b} INDO/S calculations of PTCAI absorption spectra (including $S_1 \rightarrow S_0$ and $T_1 \rightarrow T_0$ transitions) were reported by Sadrai *et al.*¹⁹

Hitherto, the analysis focused on the comparison of NTCA and PTCA has been quite limited. Few exceptions exist; Jayaraman *et al.* studied the pressure effect on the Raman and absorption spectra,²⁰ and Kowalsky *et al.* reported application in photoelectronic devices.²¹ A comparison based on the electronic structure has not yet been reported.

In this study, we calculated the electronic structure of naphthalene, NDCAI, NTCA, NTCAI, and PTCAI, focusing on the relation between the size of the π -conjugation and the absorption spectra.

2. Experimental Section

(i) Preparation and Identification of the Dyes. *N,N'*-Bis-(*p*-(ethoxycarbonyl)phenyl)-1,4,5,8-naphthalenebis(dicarboximide) (*p*-COOC₂H₅-C₆H₄-NTCAI; **6**). *p*-COOC₂H₅-C₆H₄-NTCAI was synthesized by heating a mixture of purified 1,4,5,8-tetracarboxynaphthalene and *p*-((ethoxycarbonyl)amino)benzoic acid in acetic acid at 113 °C for 7 h under stirring.

The product was analyzed and identified by C. H. analyses, HPLC, and NMR spectra: ¹H NMR ((CD₃)₂SO) δ (ppm) 1.41 (t, 6H), 4.42 (q, 4H), 7.63 (d, 2H), 8.14 (d, 2H), 8.75 (s, 4H).

N,N'-Bis(2-ethylhexyl)-3,4,9,10-perylenebis(dicarboximide) (*n*-C₄H₉(C₂H₅)-CHCH₂-PTCAI). *n*-C₄H₉(C₂H₅)-CHCH₂-PTCAI was synthesized by heating a mixture of 3,4,9,10-perylenetetracarboxylic dianhydride, 2-ethylhexylamine hydrochloride, anhydrous zinc acetate, and imidazole in quinoline at 190–200 °C for 5 h under stirring: yield 94%.

The crude product was purified by column chromatography (SiO₂, CHCl₃): mp > 300 °C; mass spectrum, *m/e* 614 (M⁺). Anal. Calcd for C₄₀H₄₂N₂O₄: C, 78.15; H, 6.89; N, 4.56. Found: C, 78.05; H, 7.34; N, 4.52.

(ii) Spectroscopic Measurements. The dyes were dissolved in solvents to give a 5.69×10^{-5} M *p*-COOC₂H₅-C₆H₄-NTCAI DMSO solution and a 1.10×10^{-5} M *n*-C₄H₉(C₂H₅)-CHCH₂-PTCAI CHCl₃ solution. The solutions were transferred to 1 cm wide cells and spectra were collected with a Shimadzu spectrophotometer (UV-3100S) and a Hitachi spectrophotometer (U-3400).

3. Calculations

The molecular geometries of the naphthalene, NDCAI, NTCA, NTCAI, and PTCAI (Figure 3) were optimized by the AM1 method.²² Spectral calculations were performed using the INDO/S method (modified to perform spectral calculations).⁵ The electronic repulsion integral was determined from the Nishimoto–Mataga formula.²³ All SCF calculations were executed at the closed-shell Hartree–Fock level (HF). Configuration interaction (CI) calculations included single excited configurations from the ground state, 35 (occupied) \times 35 (virtual). When the sum of the occupied and/or virtual orbitals amounted to less than 35, all orbitals were included in the CI calculation.

4. Results and Discussion

The calculated transitions are shown in Table 1 (for naphthalene and NDCAI), Table 2 (for NTCA and NTCAI), and Table 3 (for PTCAI). The observed absorption spectra are shown in Figure 1 for *p*-COOC₂H₅-C₆H₄-NTCAI (**6**) and in Figure 2 for *n*-C₄H₉(C₂H₅)-CHCH₂-PTCAI.

(i) Absorption Spectra of Naphthalene and NDCAI. For the naphthalene (**1**), the observed and calculated absorption spectra are in excellent agreement for both the absorption wavelength (λ_{\max}) and the intensity. The calculated 312 nm transition (B₃₀, *x*-direction) corresponds to the observed low-

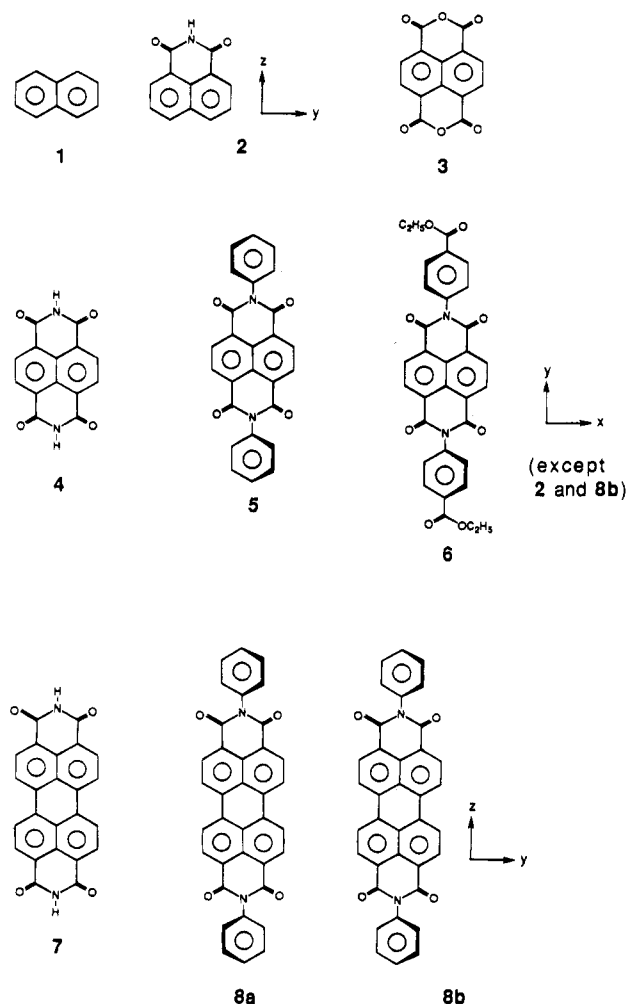


Figure 3. Calculated molecules: naphthalene (1), NDCAI (2), NTCA (3), NTCAI (4), *trans*-C₆H₅-NTCAI (5), *p*-COOC₂H₅-C₆H₄-NTCAI (6), PTCAI (7), *trans*-C₆H₅-PTCAI (8a), *cis*-C₆H₅-PTCAI (8b).

TABLE 1: Observed and Calculated Absorption Spectra of Naphthalene and NDCAI

	observed		calculated (INDO/S)		
	λ_{\max} (nm)	ϵ_{\max}	λ_{\max} (nm)	f^a	transition property
naphthalene (1) (D_{2h})	311 ^b	250	312	0.004	B _{3u} (x) (π - π^*)
	275	5600	294	0.148	B _{2u} (y) (π - π^*)
	221	117000	234	1.645	B _{3u} (x) (π - π^*)
NDCAI (2) (C_{2v})			368	0.001	B ₁ (x) (n- π^*)
			352	0.000	A ₂ (n- π^*)
	331 ^c	9800	328	0.404	A ₁ (z) (π - π^*)
	342	9300	323	0.030	B ₂ (y) (π - π^*)

^a Oscillator strength. ^b Reference 24. ^c Reference 17a.

intensity 311 nm band,²⁴ and the calculated 294 nm transition (B_{2u}, *y*-direction) corresponds to the observed high-intensity 275 nm band²⁴ (Table 1). This calculated result is almost in agreement with the previously reported INDO/S calculation (308 nm ($f = 0.002$), 265 nm ($f = 0.148$)).^{5b} But the two calculated results are slightly different; the reason for the discrepancy should be the difference of the CI size.

For NDCAI (2), both π - π^* and n- π^* transitions appeared in the calculation. The calculation shows two π - π^* transitions, one at 328 nm (A₁, *z*-direction) with high intensity ($f = 0.404$) and the other at 323 nm (B₂, *y*-direction) with low intensity ($f = 0.030$) (Table 1). The corresponding observed bands are at 342 and 331 nm.^{17a} The assignment of the NDCAI transition band was previously reported by Bigotto *et al.*, the observed

342 nm absorption band was assigned B₂ symmetry, and the 331 nm band was assigned A₁ symmetry, by comparing with the INDO/S-CI calculated values (B₂, 305 nm ($f = 0.021$); A₁, 290 nm ($f = 0.430$)).^{17a} Furthermore, the detailed transition scheme of NDCAI (NH of NDCAI is replaced by O), whose calculated transition properties are similar to those of NDCAI, was analyzed by comparison of its MCD spectrum and CNDO/S-CI calculation (B₂, 313 nm ($f = 0.004$); A₁, 306 nm ($f = 0.210$)). Their results show that the 300–350 nm absorption bands contain two electronic transitions and their vibronic progressions.^{13a} Although the calculated intensities of the two transitions are quite different relative to those of the observed spectrum (both in our result and in previous reports,^{13a,17a} see Table 1), the reason for the disagreement is the same as for NTCA and NTCAI and will be discussed in the next section. This calculated result is in good agreement with previous reports,^{13a,17a} except for the positions of two transitions (the absorption wavelength of the B₂ transition is longer than that of the A₁ transition in previous calculations,^{13a,17a} which is opposite to our results). The reason might be the limited CI size (30–50 configurations S-CI) in previous calculations.^{13a,17a}

Two n- π^* transitions of NDCAI appear in the 352–368 nm region according to the calculation, but because of their low intensity they are not observed (Table 1).

(ii) **Absorption Spectra of NTCA and NTCAIs.** For the π - π^* transitions, the calculated λ_{\max} of NTCA (3) and that of various N-substituted NTCAIs (4–6) were almost the same, indicating that there is a negligible substituent effect. The calculated 336–345 nm (B_{2u}, *y* (long)-direction) transition had high intensity, and the 334–338 nm (B_{3u}, *x* (short)-direction) transition had low intensity (Table 2). The observed absorption spectrum of *p*-COOC₂H₅-C₆H₄-NTCAI (6) is shown in Figure 1 ($\lambda_{\max} = 382, 361, 344$ (shoulder) nm). Although there is no experimental assignment for NTCAIs 4–6, it would be useful to refer to the assignment for NTCA (3), which shows similar features in the calculated spectra due to the very small substituent effect. In the observed absorption and MCD spectra already reported by Yamaguchi *et al.*,^{13a} the absorption spectrum of NTCA consists of three peaks and one shoulder. The MCD spectrum chart shows two positive and two negative peaks; therefore, Yamaguchi *et al.* concluded that these bands contain two electronic transitions and their vibronic progressions.^{13a} Given the assignment of the NTCA transition and on the basis of the fact that our calculation gives two bands, the three observed absorption bands of *p*-COOC₂H₅-C₆H₄-NTCAI may correspond to the calculated electronic transitions at 337 and 336 nm²⁵ and one of their vibronic progressions. Although the calculated intensities of the transitions at 337 and 336 nm are quite different relative to the observed peaks in Figure 1, accuracy in the calculation might be limited. When two transitions are very close in energy, there is a possibility of intensity borrowing and mixing with their vibronic progressions. These higher order properties are still far from the current level of calculation.²⁶ Yamaguchi *et al.* already reported the CNDO/S-calculated result for NTCA (B_{2u}, 322 nm ($f = 0.287$); B_{3u}, 318 nm ($f = 0.034$)).^{13a} Our INDO/S and his CNDO/S results are almost in agreement; the small discrepancy between the two methods may come from the difference of the calculation methods and the CI size.

The n- π^* transitions appeared in the calculation at wavelengths in the 339–409 nm region but with such low intensities (Table 2) that they are not observed (Figure 1).

(iii) **Absorption Spectra of PTCAIs.** For the π - π^* transitions, PTCAI (7) and the *N,N'*-diphenyl substituted molecule C₆H₅-PTCAI (8) show almost the same λ_{\max} , the 441

TABLE 2: Calculated Absorption Spectra of NTCA and NTCAIs (INDO/S)

transition property ^a	NTCA (3) (<i>D</i> _{2h})		NTCAI (4) (<i>D</i> _{2h})		<i>trans</i> -C ₆ H ₅ -NTCAI ^c (5) (<i>D</i> ₂)		<i>p</i> -COOC ₂ H ₅ -C ₆ H ₄ -NTCAI ^c (6) (<i>C</i> ₂)	
	λ_{\max} (nm)	<i>f</i> ^b	λ_{\max} (nm)	<i>f</i>	λ_{\max} (nm)	<i>f</i>	λ_{\max} (nm)	<i>f</i>
B _{3g} (n- π^*)	374	0.000	385	0.000	409	0.006	404	0.004
B _{1u} (z) (n- π^*)	371	0.001	379	0.001	406	0.002	401	0.002
B _{2g} (n- π^*)	359	0.000	364	0.000	381	0.001	380	0.001
A _u (n-p*)	358	0.000	361	0.000	379	0.000	378	0.000
(n- π^*) ^d							339	0.000
(n- π^*) ^d							339	0.000
B _{2u} (y) (π - π^*)	340 ^e	0.609	345	0.620	336	0.829	336 ^f	0.960
B _{3u} (x) (π - π^*)	334 ^e	0.099	337	0.091	338	0.030	337 ^f	0.049

^a Transition symmetries were assigned in the *D*_{2h} point group. ^b Oscillator strength. ^c Optimized dihedral angles between the phenyl ring and the NTCAI plane are $\sim 50^\circ$. ^d O(=COC₂H₅) lone pair (n) to phenyl ring π -orbital transition. ^e Observed: λ_{\max} (ϵ) 351 nm (10 000), 322 nm (8500) (ref 13a), see the text. ^f Observed: λ_{\max} (ϵ) 382 nm (23 600), 361 nm (22 900), 344 nm (shoulder) (Figure 1), see the text.

TABLE 3: Calculated Absorption Spectra of PTCAIs (INDO/S)

transition property ^a	PTCAI (7) (<i>D</i> _{2h})		<i>trans</i> -C ₆ H ₅ -PTCAI (8a) ^c (<i>D</i> ₂)		<i>cis</i> -C ₆ H ₅ -PTCAI (8b) ^c (<i>C</i> _{2v})	
	λ_{\max} (nm)	<i>f</i> ^b	λ_{\max} (nm)	<i>f</i>	λ_{\max} (nm)	<i>f</i>
B _{2u} (y) (π - π^*)	441	1.258	441 ^d	1.411	441 ^d	1.412
B _{1u} (z) (n- π^*)	373	0.001	396	0.002	396	0.000
B _{3g} (n- π^*)	373	0.000	396	0.005	396	0.007
A _u (n- π^*)	355	0.000	371	0.000	371	0.002
B _{2g} (n- π^*)	355	0.000	371	0.002	371	0.000
B _{1g} (π - π^*)	347	0.000	348	0.000	348	0.000
B _{3u} (x) (π - π^*)	344	0.022	344	0.015	344	0.015

^a Transition symmetries were assigned in the *D*_{2h} point group. ^b Oscillator strength. ^c Optimized dihedral angles between the phenyl ring and the PTCAI plane are $\sim 50^\circ$. ^d Observed (for 8): λ_{\max} (ϵ) 525 nm (50 000), 489 nm (32 000), 458 nm (13 000) (ref 27).

nm (B_{2u}, y (long)-direction) transition has a high intensity, the 347–348 nm (B_{1g}) transition is forbidden, and the 344 nm (B_{3u}, x (short)-direction) transition has a low intensity (Table 3). The *trans*- and *cis*-*N,N'*-diphenyl-substituted molecules (8a and 8b) show almost the same transition properties, because the transition properties are mainly determined by the PTCAI moiety. Sadrai *et al.* already reported the INDO/S-calculated result of *N,N'*-dimethyl-PTCAI (438 nm (*f* = 1.281));¹⁹ his result (including higher transitions) is in complete agreement with our calculation.

The observed LD and CD spectra of PTCAI show that three peaks of the absorption spectrum consist of one electronic transition and its vibronic progressions.^{14c} The observed bands of C₆H₅-PTCAI (8) are at 525, 489, and 458 nm (λ_{\max});²⁷ the energy intervals of the three bands are 1400 and 1380 cm⁻¹; and the difference of 20 cm⁻¹ can be attributed to the vibrational anharmonicity. From the calculations, only one intense electronic transition emerges (441 nm); the next intense electronic transition appears at ~ 100 nm shorter wavelength. Generally, when the interval of two electronic transition energies is larger than the vibrational frequencies, the mixing of the two electronic transitions is negligible. In such instances, the absorption spectrum may emerge as one of the following two cases: (1) a single peak for each electronic transition appears, or (2) several peaks appear as a result of one electronic transition and its vibronic progressions. For PTCAI, the calculated separation between the longest π - π^* transition and the next one amounts to ~ 100 nm (~ 6000 cm⁻¹); this is too large to be vibrational frequencies. Therefore, the observed three bands may be assigned to one electronic transition (525 nm) and its vibronic progressions (489, 458 nm); *i.e.*, the observed 525 nm absorption band corresponds to the calculated 441 nm transition²⁸ (see the band with a high intensity in Table 3).

For the calculated transition at 344 nm²⁸ (B_{3u}, *x*-direction), no experimental assignment has previously been reported. In

TABLE 4: Detail of π - π^* Transition Property for Naphthalene, NDCAI, NTCAI, and PTCAI (INDO/S)

	λ_{\max} (nm)	<i>f</i> ^a	transition property ^b		
naphthalene (1)	312	0.004	B _{3u} (x)	-0.741 {(HOMO,24)→26}	(39090) ^f
				0.652 {23→(LUMO,25)}	(40400)
	294	0.148	B _{2u} (y)	-0.921 {HOMO→LUMO}	(38920)
NDCAI (2)	328	0.404	A ₁ (z) ^d	0.956 {(HOMO,36)→(LUMO,37)}	(33900)
	323	0.030	B ₂ (y) ^d	0.872 {35→LUMO}	(36830)
				-0.521 {HOMO→38}	(39280)
NTCAI (4)	345	0.620	B _{2u} (y)	0.970 {(HOMO,48)→(LUMO,49)}	(31580)
	337	0.091	B _{3u} (x)	0.860 {47→LUMO}	(34340)
				-0.467 {HOMO→51}	(40160)
PTCAI (7)	441 ^e	1.258	B _{2u} (y)	-0.981 {(HOMO,70)→(LUMO,71)}	(23970)
	347	0.000	B _{1g}	0.739 {69→LUMO}	(33500)
				-0.548 {HOMO→74}	(35460)
	344 ^f	0.022	B _{3u} (x)	0.701 {68→LUMO}	(35740)
				0.583 {HOMO→75}	(37330)
	315	0.000	A _g	0.935 {HOMO→72}	(34270)
	279	0.000	A _g	0.939 {67→LUMO}	(37870)

^a Oscillator strength. ^b Excitations having the CI coefficient larger than 0.4 are shown. ^c Value in parentheses shows generated configuration (a → b) excitation energy ($\Delta E(a \rightarrow b)$, cm⁻¹). ^d In NDCAI, *z*-axis corresponds to *y*-axis in other molecules. Also, *y*-axis corresponds to *x*-axis (Figure 3).²⁹ ^e In Figure 8, this transition is shown. ^f In Figure 9, this transition is shown.

a similar molecule (*n*-C₄H₉(C₂H₅)-CHCH₂-PTCAI), the calculated 344 nm transition can correspond to the 370 nm (ϵ = 4000) absorption band (Figure 2).

The n- π^* transitions appear in the 355–396 nm region in the calculation, but all the transitions have a low intensity (Table 3); therefore, they are not observed (Figure 2).

(iv) Comparison of Absorption Spectra (π - π^* Transition). The π - π^* transition properties of naphthalene (1), NDCAI (2), NTCAI (4), and PTCAI (7) are summarized in Table 4. The frontier orbital diagram of these molecules is drawn in Figure 4. The frontier orbitals of naphthalene (Figure 5), NDCAI (Figure 6), NTCAI (Figure 7), and PTCAI (Figure 8) are also displayed. As shown in Table 4, from 1 to 7, the high intensity *y*-directed transition (*y*-axis corresponds to *z*-axis of NDCAI (2), Figure 3)²⁹ shows a remarkable bathochromic shift; on the other hand, the low-intensity *x*-directed transition (*x*-axis corresponds to *y*-axis of NDCAI (2), Figure 3)²⁹ shows only a small bathochromic shift.

The intense *y*-directed transitions are mainly HOMO → LUMO excitations (Table 4). In Figure 9, the transition energy (E_{\max} , reciprocal value of λ_{\max}) and the HOMO → LUMO excitation energy ($\Delta E(\text{HOMO} \rightarrow \text{LUMO})$) of each molecule are shown. The transition energy (E_{\max}) and the excitation energy ($\Delta E(\text{HOMO} \rightarrow \text{LUMO})$) decrease in a similar way as the amount of π -conjugation increases. Therefore, the bathochromic shifts from naphthalene (1) to PTCAI (7) are the result of the HOMO → LUMO excitation energy change. The HOMO → LUMO excitation energy ($\Delta E(\text{HOMO} \rightarrow \text{LUMO})$) is expressed by using

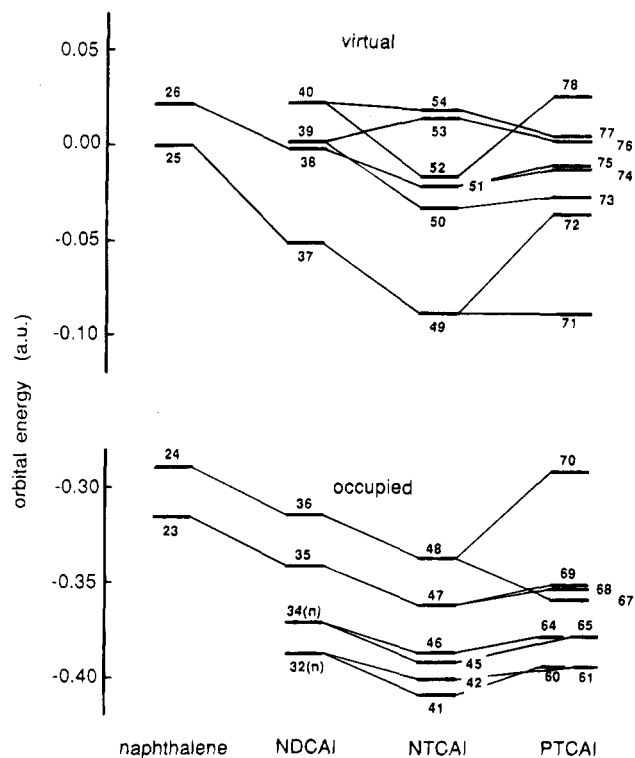


Figure 4. Orbital energies (atomic unit) of naphthalene, NDCAI, NTCAI, and PTCAI (INDO/S).

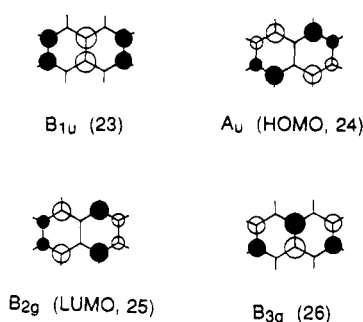


Figure 5. Frontier molecular orbitals of naphthalene (INDO/S).

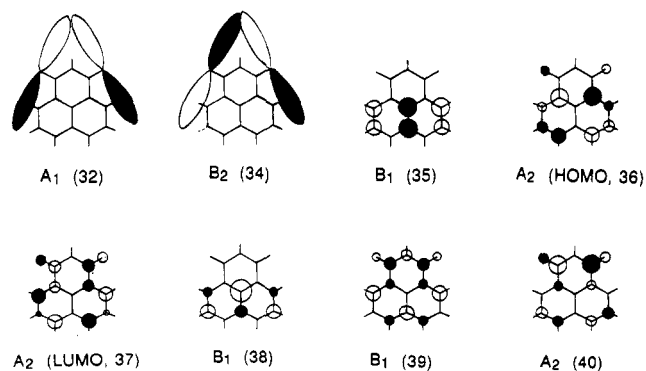


Figure 6. Frontier molecular orbitals of NDCAI (INDO/S).

the orbital energy difference ($\Delta\epsilon$) and the electronic interaction terms J and K ,

$$\Delta E(\text{HOMO} \rightarrow \text{LUMO}) = \Delta\epsilon(\text{HOMO, LUMO}) - J(\text{HOMO, LUMO}) + 2K(\text{HOMO, LUMO})$$

where J is the Coulomb integral and K is the exchange integral. The calculated HOMO \rightarrow LUMO excitation energies and each

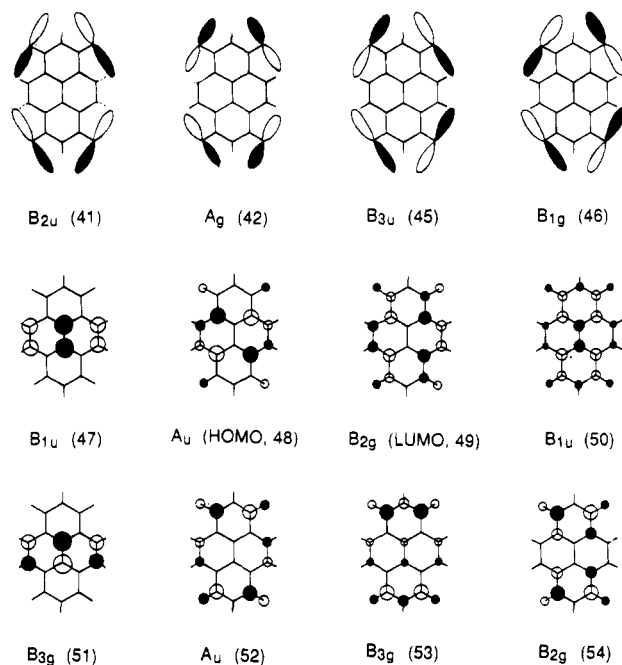


Figure 7. Frontier molecular orbitals of NTCAI (INDO/S).

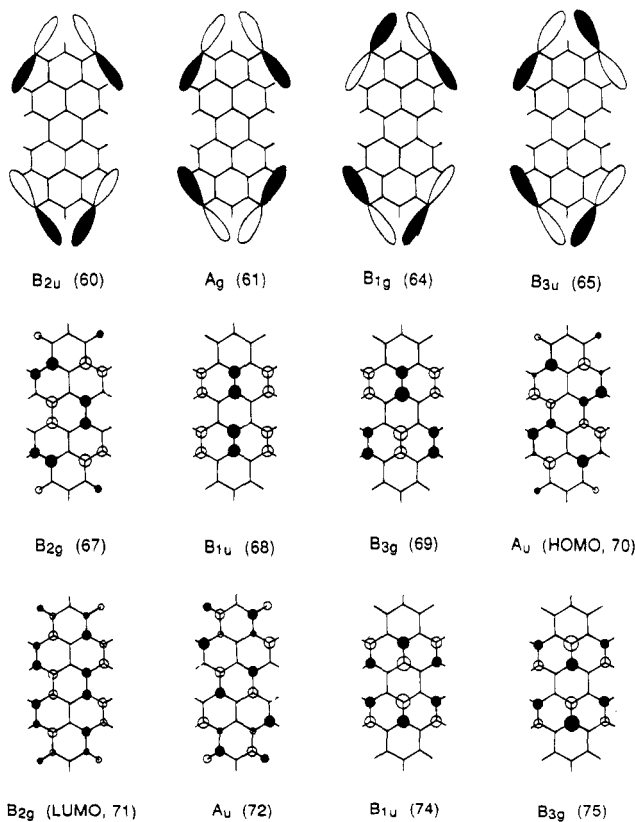


Figure 8. Frontier molecular orbitals of PTCAI (INDO/S).

component ($\Delta\epsilon$, J , and $2K$) of naphthalene, NDCAI, NTCAI, and PTCAI are shown in Table 5. The electronic interaction term ($J(\text{HOMO, LUMO}) - 2K(\text{HOMO, LUMO})$) decreases only slightly, while the orbital energy gap ($\Delta\epsilon(\text{HOMO, LUMO})$) decreases remarkably (almost as much as the excitation energy change, $\Delta E(\text{HOMO} \rightarrow \text{LUMO})$). Therefore, the transition energy shift is attributed to the HOMO and LUMO energy levels.

In Figures 5–7, the LUMO is delocalized for both naphthalene and the carboxylic anhydride moiety, while the HOMO is almost localized in the naphthalene ring. As shown in Figure 4, from naphthalene to NDCAI to NTCAI, the LUMO level

TABLE 5: Detail of HOMO \rightarrow LUMO Excitation for Naphthalene, NDCAI, NTCAI, and PTCAI (INDO/S)

	$\Delta E(\text{HOMO} \rightarrow \text{LUMO})^a$ (cm^{-1})	$\Delta \epsilon(\text{HOMO}, \text{LUMO})^b$ (cm^{-1})	$J(\text{HOMO}, \text{LUMO})^c$ (cm^{-1})	$2K(\text{HOMO}, \text{LUMO})^d$ (cm^{-1})	$J(\text{HOMO}, \text{LUMO}) - 2K(\text{HOMO}, \text{LUMO})$ (cm^{-1})
naphthalene (1)	38 920	63 430	41 200	16 690	24 510
NDCAI (2)	33 900	58 060	36 340	12 180	24 160
NTCAI (4)	31 580	54 890	34 350	11 040	23 310
PTCAI (7)	23 970	44 530	28 860	8 300	20 560

^a Excitation energy. ^b Difference of orbital energy. ^c Coulomb integral. ^d Exchange integral.

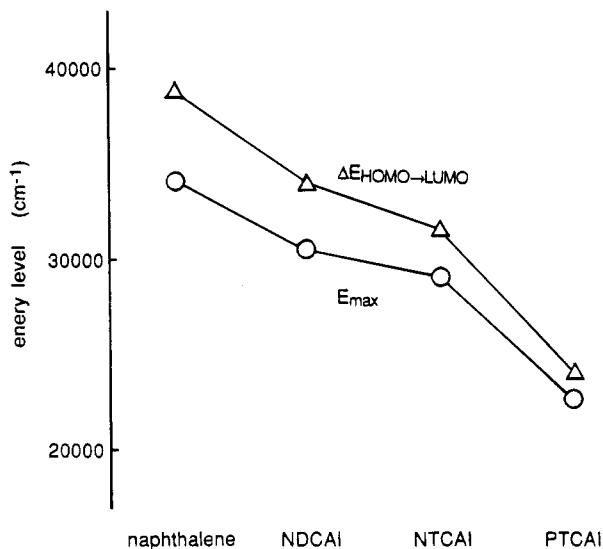


Figure 9. $\pi-\pi^*$ transition energy with large intensity (E_{max}) and $\Delta E(\text{HOMO} \rightarrow \text{LUMO})$ of naphthalene, NDCAI, NTCAI, and PTCAI (INDO/S).

goes down more than the HOMO level does, since the HOMO is localized. This situation produces the decrease of the HOMO–LUMO gap (Figure 4).

On the other hand, the bathochromic shift from NTCAI to PTCAI stems from the number of naphthalene units. That is, PTCAI has two naphthalene moieties; therefore, the HOMO of one naphthalene ring and the HOMO of other naphthalene ring interact and generate two orbitals (67 and HOMO:70). Similarly LUMOs generate two orbitals (LUMO:71 and 72) (Figures 4 and 8). As a result, four transitions corresponding to the HOMO \rightarrow LUMO transitions of two naphthalene moieties appear for PTCAI. These are the 441, 315, and 279 nm transitions (Table 4); the fourth and the shortest one, less than 225 nm, is not shown in Table 4. The HOMO and LUMO of the naphthalene have large lobes on the 1,4,5,8-positions (connecting points at the perylene, Figure 5). Therefore increasing the number of naphthalene rings from NTCAI to PTCAI causes these orbitals to interact and produce a large splitting of the bonding type (67 and LUMO:71, B_{2g} symmetry in Figures 4 and 8) and the antibonding type (HOMO:70 and 72, A_u symmetry in Figures 4 and 8) orbitals. For PTCAI, the 441 nm transition (mainly HOMO \rightarrow LUMO excitation) is an allowed transition by the orbital symmetry. Therefore, from NTCAI to PTCAI, a large bathochromic shift has appeared (Table 4). In other words, the bathochromic shift of the high-intensity y -directed transition can be explained by the increase of the π -conjugation size along the y -axis (Figures 4–9).

In contrast, the low-intensity x -directed $\pi-\pi^*$ transitions show a small bathochromic shift (Table 4). These transitions consist of the (HOMO $- m$) \rightarrow LUMO ($m = 1$ for naphthalene, NDCAI, and NTCAI and 2 for PTCAI) and HOMO \rightarrow (LUMO $+ n$) ($n = 1$ for naphthalene and NDCAI, 2 for NTCAI, and 4 for PTCAI) excitations (Table 4). The transition energy (E_{max}) and the excitation energy ($\Delta E(a \rightarrow b)$) of these generated

TABLE 6: Detail of $n-\pi^*$ Transition Property for NDCAI, NTCAI, and PTCAI (INDO/S)

	λ_{max} (nm)	f^a	transition property ^b	
NDCAI (2)	368	0.001	$B_1(x)$	0.697 {34 \rightarrow (LUMO,37)} (39 240) ^c
				0.477 {34 \rightarrow 40} (51 710)
	352	0.000	A_2	0.620 {32 \rightarrow LUMO} (42 350)
				0.465 {34 \rightarrow 39} (50 490)
				0.431 {32 \rightarrow 40} (55 250)
NTCAI (4)	385	0.000	B_{3g}	-0.663 {46 \rightarrow (LUMO,49)} (37 990)
				-0.464 {45 \rightarrow 52} (53 520)
	379	0.001	$B_{1u}(z)$	-0.635 {45 \rightarrow LUMO} (39 490)
				-0.490 {46 \rightarrow 52} (52 120)
	364	0.000	B_{2g}	-0.598 {42 \rightarrow LUMO} (40 550)
				-0.433 {41 \rightarrow 52} (57 100)
				-0.401 {45 \rightarrow 50} (51 520)
	361	0.000	A_u	0.570 {41 \rightarrow LUMO} (42 880)
				0.438 {42 \rightarrow 52} (55 310)
				0.428 {46 \rightarrow 50} (50 000)
PTCAI (7)	373	0.001	$B_{1u}(z)$	0.531 {65 \rightarrow (LUMO,71)} (41 930)
				-0.476 {64 \rightarrow 72} (51 690)
	373	0.000	B_{3g}	-0.530 {64 \rightarrow LUMO} (41 980)
				-0.477 {65 \rightarrow 72} (51 640)
	355	0.000	A_u	-0.470 {60 \rightarrow LUMO} (44 910)
				-0.425 {61 \rightarrow 72} (54 670)
	355	0.000	B_{2g}	0.465 {61 \rightarrow LUMO} (44 620)
				0.431 {60 \rightarrow 72} (54 840)

^a Oscillator strength. ^b Excitations having the CI coefficient larger than 0.4 are shown. ^c Value in parentheses shows generated configuration (a \rightarrow b) excitation energy ($\Delta E(a \rightarrow b)$, cm^{-1}).

configurations are almost unchanged (Table 4). These trends in excitation energies are also explained by the orbital energy differences. The orbital energy change of the HOMO $- 1$ and LUMO $+ 1$ (especially LUMO $+ 1$, at naphthalene) orbitals is smaller than that of the HOMO and LUMO (Figure 4), because these orbitals are localized only in naphthalene rings (Figures 5–8). The HOMO $- 1$ and LUMO $+ 1$ orbitals of the naphthalene have no lobes on the 1,4,5,8-positions (Figure 5). Therefore for PTCAI, two almost degenerate orbitals appear (68, 69 and 74, 75; Figures 4 and 8); thus, two transitions appear at 344 nm (B_{3u} , allowed) and 347 nm (B_{1g} , forbidden), and two more transitions appear at < 225 nm (not shown in Table 4).

(v) Comparison of Absorption Spectra ($n-\pi^*$ Transition). The $n-\pi^*$ transition properties of NDCAI (2), NTCAI (4), and PTCAI (7) are summarized in Table 6. For the $n-\pi^*$ transitions, the transition energies are almost the same in all molecules. These transitions are described by several configurations generated by excitations from the carbonyl O atom lone pair to the LUMO and other virtual orbitals (Table 6 and Figures 6–8). The $n-\pi^*$ transition energies of NDCAI, NTCAI, and PTCAI are almost the same (Table 6), which is probably due to the nearly equal excitation energy of the generated configurations (the last column of Table 6).

5. Conclusion

The absorption spectra of naphthalene, NDCAI, NTCAI, and PTCAI were studied. The observed absorption spectrum shapes of NTCAI and PTCAI seem similar apart from some band shifts. Calculations showed that NDCAI and NTCAI have two $\pi-\pi^*$

electronic transitions (each transition vector is perpendicular) in the near energy region. Therefore, the observed spectra are understood as the mixing of two electronic transitions and their vibronic progressions. On the other hand, in PTCAI the observed absorption spectrum consists of one electronic transition and its vibronic progressions.

The mechanism of the absorption wavelength shift from naphthalene, NDCAI, and NTCAI to PTCAI was analyzed. The $\pi-\pi^*$ transitions with high intensity in the direction of the long axis show a remarkable bathochromic shift, having mainly HOMO \rightarrow LUMO excitation properties. The bathochromic shift is explained by the decrease of the orbital energy gap. Specifically, the bathochromic shift is the result of the π -conjugation size. The $\pi-\pi^*$ transitions with low intensity in the direction of short axis show only a small bathochromic shift, and this shift can be explained by the small change of the orbital energy gaps. Thus, the π -conjugation size effect in these two $\pi-\pi^*$ transitions is different in details.

The $n-\pi^*$ transitions in NDCAI, NTCAI, and PTCAI were also analyzed. The absorption wavelengths of the $n-\pi^*$ transitions are kept at almost the same levels.

Acknowledgment. The authors thank Dr. T. Hirahara for discussion, Ms. Y. Nakajima for absorption spectrum observation, and Professor M. C. Zerner for the release of the ZINDO program.

References and Notes

- (1) Orchin, M.; Jaffé, H. H. *Symmetry, Orbitals, and Spectra*; John Wiley & Sons: New York, 1971.
- (2) Griffiths, J. *Colour and Constitution of Organic Molecules*; Academic Press: London, 1976.
- (3) Fabian, J.; Hartmann, H. *Light Absorption of Organic Colorants*; Springer-Verlag: Berlin, 1980.
- (4) Nishimoto, K. *Bull. Chem. Soc. Jpn.* **1993**, *66*, 1876.
- (5) (a) Ridley, J. E.; Zerner, M. C. *Theor. Chim. Acta* **1973**, *32*, 111. (b) Ridley, J. E.; Zerner, M. C. *J. Mol. Spectrosc.* **1974**, *50*, 457. (c) Bacon, A. D.; Zerner, M. C. *Theor. Chim. Acta* **1979**, *53*, 21. (d) Zerner, M. C.; Loew, G. H.; Kirchner, R. F.; Mueller-Westerhoff, U. T. *J. Am. Chem. Soc.* **1980**, *102*, 589.
- (6) Adachi, M.; Nakamura, S. *Dyes Pigm.* **1991**, *17*, 287.
- (7) (a) Kubo, Y.; Yoshida, K.; Adachi, M.; Nakamura, S.; Maeda, S. *J. Am. Chem. Soc.* **1991**, *113*, 2868. (b) Adachi, M.; Murata, Y.; Nakamura, S. *J. Am. Chem. Soc.* **1993**, *115*, 4331. (c) Adachi, M.; Murata, Y.; Nakamura, S. *J. Org. Chem.* **1993**, *58*, 5238.
- (8) (a) Adachi, M.; Yoneyama, M.; Nakamura, S. *Langmuir* **1992**, *8*, 2240. (b) Nakamura, S.; Flamini, A.; Fares, V.; Adachi, M. *J. Phys. Chem.* **1992**, *96*, 8351.
- (9) Adachi, M.; Nakamura, S. *J. Phys. Chem.* **1994**, *98*, 1796.
- (10) Hirahara, T.; Nakamura, T.; Aoyama, Y.; Maeda, S. (Mitsubishi Kasei Corp.) EP 263,705-B1, June 30, 1993.
- (11) Klebe, G.; Graser, F.; Hädicke, E.; Berndt, J. *Acta Crystallogr.* **1989**, *B45*, 69.
- (12) (a) Popovic, Z. D.; Loutfy, R. O.; Hor, A.-M. *Can. J. Chem.* **1985**, *63*, 134. (b) Duff, J.; Hor, A. M.; Melnyk, A. R.; Teney, D. *Proc. SPIE-Int. Soc. Opt. Eng.* **1990**, *1253 (Hard Copy Print. Mater., Media, Process)*, 183.

- (13) (a) Yamaguchi, H.; Kitano, K.; Toyoda, K.; Baumann, H. *Spectrochim. Acta* **1982**, *38A*, 261. (b) Bondarenko, E. F.; Shigalevskii, V. A.; Yagai, G. A. *Zh. Org. Khim.* **1982**, *18*, 610.
- (14) (a) Rademacher, A.; Märkle, S.; Langhals, H. *Chem. Ber.* **1982**, *115*, 2927. (b) Sadrai, M.; Bird, G. R. *Opt. Commun.* **1984**, *51*, 62. (c) Johansson, L. B.-Å.; Langhals, H. *Spectrochim. Acta* **1991**, *47A*, 857.
- (15) (a) Ilmet, I.; Berger, S. A. *J. Phys. Chem.* **1967**, *71*, 1534. (b) Sep, W. J.; Verhoeven, J. W.; de Boer, Th. J. *Tetrahedron* **1975**, *31*, 1065. (c) Schroff, L. G.; Zsom, R. L. J.; van der Weerd, A. J. A.; Schrier, P. I.; Geerts, J. P.; Nibbering, N. M. M.; Verhoeven, J. W.; de Boer, Th. J. *Recl. Trav. Chim. Pays-Bas* **1976**, *95*, 89. (d) Kheifets, G. M.; Marttyushina, N. V.; Mikhailova, T. A.; Khromov-Borisov, N. V. *Zh. Org. Khim.* **1977**, *13*, 1262. (e) Zsom, R. L. J.; Schroff, L. G.; Bakker, C. J.; Verhoeven, J. W.; de Boer, Th. J.; Wright, J. D.; Kuroda, H. *Tetrahedron* **1978**, *34*, 3225.
- (16) Zhong, C. J.; Kwan, W. S. V.; Miller, L. L. *Chem. Mater.* **1992**, *4*, 1423.
- (17) (a) Bigotto, A.; Galasso, V.; Distefano, G.; Modelli, A. *J. Chem. Soc., Perkin Trans. 2* **1979**, 1502. (b) Celnik, K.; Jankowski, Z.; Stolarski, R. *Pol. J. Chem.* **1983**, *57*, 817. (c) Pardo, A.; Campanario, J.; Poyato, J. M. L.; Camacho, J. J.; Reyman, D.; Martin, E. *THEOCHEM* **1988**, *166*, 463. (d) Xuhong, Q.; Zhenghua, Z.; Kongchang, C. *Dyes Pigm.* **1989**, *11*, 13. (e) Alexiou, M. S.; Tychopoulos, V.; Ghorbanian, S.; Tyman, J. H. P.; Brown, R. G.; Brittain, P. I. *J. Chem. Soc., Perkin Trans. 2* **1990**, 837. (f) Malkes, L. Ya.; Minakova, R. A.; Bedrik, A. I. *Zh. Prikl. Spektrosk.* **1991**, *55*, 820.
- (18) (a) Lukác, I.; Langhals, H. *Chem. Ber.* **1983**, *116*, 3524. (b) Langhals, H. *Chem. Ber.* **1985**, *118*, 4641. (c) Langhals, H.; Fünfschilling, J.; Glatz, D.; Zschokke-Gränacher, I. *Spectrochim. Acta* **1988**, *44A*, 311. (d) Langhals, H.; Demmig, S.; Huber, H. *Spectrochim. Acta* **1988**, *44A*, 1189. (e) Demmig, S.; Langhals, H. *Chem. Ber.* **1988**, *121*, 225. (f) Kaiser, H.; Lindner, J.; Langhals, H. *Chem. Ber.* **1991**, *124*, 529.
- (19) Sadrai, M.; Hadel, L.; Sauers, R. R.; Husain, S.; Krogh-Jespersen, K.; Westbrook, J. D.; Bird, G. R. *J. Phys. Chem.* **1992**, *96*, 7988.
- (20) Jayaraman, A.; Kaplan, M. L.; Schmidt, P. H. *J. Chem. Phys.* **1985**, *82*, 1682.
- (21) Kowalsky, W.; Rompf, C. *Teubner-Texte Phys.* **1993**, 76.
- (22) (a) Dewar, M. J. S.; Zoebisch, E. G.; Healy, E. F.; Stewart, J. J. P. *J. Am. Chem. Soc.* **1985**, *107*, 3902. (b) Stewart, J. J. P. MOPAC, Version 5; *QCPE Bull.* **1989**, *9*, 10.
- (23) (a) Nishimoto, K.; Mataga, N. *Z. Phys. Chem. (Munich)* **1957**, *12*, 335. (b) Mataga, N.; Nishimoto, K. *Z. Phys. Chem. (Munich)* **1957**, *13*, 140.
- (24) Perkampus, H.-H. *UV-VIS Atlas of Organic Compounds*, 2nd ed.; VCH: Weinheim, 1992; Part 2, pp 571.
- (25) In some cases, INDO/S calculation underestimates the absorption wavelength, especially for organic dyes and pigments. We have previously proposed the following relationship between the observed and calculated λ_{\max} : $\lambda_{\max}^{(6)} = 1.65\lambda_{\max}^{(\text{calc})} - 187$ (nm). The scaled values are 369 and 367 nm using this equation.
- (26) (a) Orlandi, G.; Siebrand, W. *J. Chem. Phys.* **1973**, *58*, 4513. (b) Canuto, S.; Zerner, M. C. *J. Am. Chem. Soc.* **1990**, *112*, 2114. (c) Negri, F.; Orlandi, G.; Zerbetto, F. *J. Chem. Phys.* **1992**, *97*, 6496.
- (27) Okawara, M.; Kitao, T.; Hirashima, T.; Matsuoka, M. *Physical Sciences Data 35, Organic Colorants*; Kodansha-Elsevier: Amsterdam, 1988; pp 246–247.
- (28) The scaled values of the C_6H_5 -PTCAI absorption wavelength are 541 and 381 nm (see ref 25).
- (29) The molecular symmetry of NDCAI is C_{2v} (others D_{2h}); thus the molecular axis is different from that of other molecules (Figure 3). In this section, the axis of NDCAI is set to be the same as that of naphthalene (D_{2h}) for ease of comparison.

JP943032F